Analysis of a Resistive-Capacitive Shunted Josephson Junction with Topologically Nontrivial Barrier Coupled to a RLC Resonator

Jules Metsebo [ID]*,1, **Boubakary Abdou** [ID]β,2, **Dianorré Tokoue Ngatcha** [ID]α,3, **Isidore Komofor Ngongiah** [ID]θ,4, **Paul Didier Kamdem Kuate** [ID]γ,5 and **Justin Roger Mboupda Pone** [ID]σ,6

*Department of Hydraulics and Water Management, National Advanced School of Engineering, University of Maroua, P.O Box 58 Maroua, Cameroon, βDepartment of Mechanical, Petroleum and Gas Engineering, National Advanced School of Mines and Petroleum Industries, University of Maroua, P.O. Box 46, Maroua, Cameroon, αLaboratory of Mechatronics, Energiatronics and Sustainable Mobility, Department of Automotive and Mechatronics Engineering, National Higher Polytechnic School of Douala, University of Douala, P.O. Box 24, 2701 Douala, Cameroon, θDepartment of Physics, Faculty of Science, University of Bamenda, P.O. Box 39 Bamenda, Cameroon, γLaboratory of Condensed Matter, Electronics and Signal Processing, Department of Physics, University of Dschang, P.O. Box 067, Dschang, Cameroon, σResearch Unit of Automation and Applied Computer (RU-AIA), Electrical Engineering Department of IUT-FV, University of Dschang, P.O. Box: 134, Bandjoun, Cameroon.

ABSTRACT This paper presents the resistive-capacitive shunted Josephson junction (RCSJJ) with a topologically nontrivial barrier (TNB) coupled to a linear RLC resonator. The rate equations describing RCSJJ with TNB coupled to the linear RLC resonator are established via Kirchhoff's current and voltage laws. The model exhibits four, two, or no equilibrium points depending on the external direct current (DC) source and the fractional parameter. The stability analysis of the equilibrium points with credit to the Routh-Hurwitz stability criterion reveals that the stability of equilibrium points depends on the DC source and the fractional parameter. Current-voltage characteristic reveals the presence of a birhythmicity zone which is sensitive to the fractional parameter m. As the fractional parameter increases, the coexistence of the resonant state is destroyed, which is followed simultaneously by the appearance of a new resonance state. Depending on initial conditions, birhythmic behaviour is characterized by the existence of a limit cycle. The projection of the phase space in the specific plane and the time evolution of charge is predicted in which the amplitude of attractors reported is sensitive to the parameter m. Lastly, with a defined fractional parameter, the amplitude of the branch locked to the resonator is greater than the unlocked branch.

INTRODUCTION

In 1962, Brian David Josephson analysed the happenings at the junction between two closely spaced superconductors, separated by an insulating barrier. If the insulating barrier is thick, the electron pairs cannot get through, but if the layer is thin enough (approximately 10 nm) there is a probability for electron pairs to the tunnel (Fujii *et al.* 2009). This effect later became known as "Josephson tunnelling". Whatever the nature of the junction, its thickness has to be comparable to or smaller than the coherence length of the two superconductors (Owen and Scalapino 1997). Otherwise, the dynamics of the respective Cooper pairs are uncorrelated.

The current that crosses the barrier is the Josephson current. The Josephson effect is based on the behaviour of a quantum parameter called phase. As a result of the fact that the barrier is thin enough, the phase of the electron wave function in one superconductor maintains a fixed relationship with the phase of the wave function in the other superconductor (Eck *et al.* 1965). This linking up of phases is called phase coherence which is the essence of the Josephson effects. Recently, the interest in Josephson physics has shifted towards junctions whose elements include topological materials Bao *et al.* (2015) which enable the specific design of the hybrid junction (Mourik *et al.* 2012).

In the literature, JJs with a TNB is a model that can display excitable mode, bistable, periodic and chaotic behaviours (Kingni *et al.* 2020). In essence, there is an interesting aspect of topological nontrivial barriers known as fractality that plays an important role in several physical phenomena such as the nuclear fusion that occurs in main progression stars like the sun and this is known as quantum tunnelling (Bee *et al.* 2008). Quantum tunnelling in JJ has been the subject of great interest because of its possible technological applications in phase qubit Nori (2008); Clarke and Wilhelm

(2008), superconducting electronic devices, ultrahigh sensitive detectors, parametric amplifiers, voltage standards and superconducting quantum interference devices for the detection of very weak magnetic fields (Kleiner *et al.* 2004; McDermott *et al.* 2004; Oladapo *et al.* 2018). In the literature, JJs based on low-critical temperature superconductors have a harmonic current phase relation (Belli *et al.* 2012). While JJs based on high critical-temperature superconductors Campi *et al.* (2021) have an unharmonic current-phase relation due to the anisotropic and multiband effects in superconductors.

The analytical and numerical analysis of JJs with unharmonic current-phase relation has been reported in the literature over the past year (Canturk and Askerzade 2013; Kingni *et al.* 2019). In the case of JJs based on topologically nontrivial barriers Veldhorst *et al.* (2012), the current-phase relation includes an additional fractional term related to the Majorana particles (Dominguez *et al.* 2012; Fu and Kane 2009). Majorana particles are particles identical to their antiparticles which are described by real value wave functions and attract considerable interest in quantum computations (Lima *et al.* 2021; Wendin 2017). Furthermore, topological supercurrents interaction and fluctuations in the multiterminal Josephson effect emerge from the quantum coherence of electron trajectories and are sensitive to changes in the external magnetic field or gate voltage (Xie and Levchenko 2019; Ramakrishnan *et al.* 2022). When superconductivity is induced at the boundary of the mesoscopic sample via the proximity effect, the universality of conductance fluctuations remains intact (Bao *et al.* 2015; Aleiner and Blanter 2002). The phenomenon of conductance fluctuations is an aspect of fractality which is based on the fractional quantum Hall effect and appears in electron systems in two-dimensional (2D) for a strong magnetic field (Wen 2006).

The contemporary presence of two frequencies for the same set of parameters, or birhythmicity, is encountered in some biochemical systems Decroly and Goldbeter (1982); Morita *et al.* (1989); Haberichter *et al.* (2001); Sosnovtseva *et al.* (2002); Abou-Jaoudé *et al.* (2011a), nonlinear electronic circuits Kadji *et al.* (2007); Zakharova *et al.* (2010); Yamapi *et al.* (2010); Ghosh *et al.* (2011); Yamapi *et al.* (2012); Yue *et al.* (2012), and extended distributed systems (Stich *et al.* 2002; Casagrande and Mikhailov 2005). The experimental observation of birhythmic systems, however, is less frequent (Hounsgaard *et al.* 1988; Geva-zatorsky *et al.* 2006; Ventura *et al.* 2007; González *et al.* 2008).

In this context, the superconducting circuit consisting of JJs coupled to a cavity Hadley *et al.* (1988); Filatrella *et al.* (1992); Ozyuzer *et al.* (2007), represents a preeminent example of a birhythmic system that is also interesting for applications. The coupling among the junctions is supposed to be provided by a resonant cavity Gross *et al.* (2013); Grib *et al.* (2006), thus when all the junctions are entrained it is essential to have a large current in the cavity such that the junctions can be entrained through the current in the resonator. The state with a large current coexists with a state at lower power, such that the two states are characterized by two different frequencies. This is the essential feature of birhythmicity, the coexistence of two attractors characterized by two different amplitudes and frequencies.

Birhythmicity is therefore a nonlocal phenomenon that cannot be investigated by linear analysis. The global stability of the two states at different frequencies of the current-voltage (IV) characteristic ascertained the birhythmic properties induced by the RLC circuit. There is evidence from simulation that at the same bias point, two frequencies appear, depending on the initial conditions. The first frequency is reached by increasing the bias current from

zero on the Josephson supercurrent, while the second is obtained by decreasing the current from high values on the resistive McCumber branch, such that the selection of the frequency displayed is thus determined by the initial conditions (Yamapi and Filatrella 2014). The features of the IV depend upon other factors such as the number of JJs and the features of the resonator (Grib *et al.* 2006). Also, heating effects are believed to be relevant for coherent radiation Wang *et al.* (2010), as well as coupling through charge transfer through the Josephson channel (Ovchinnikov and Kresin 2013).

The JJ can be considered a birhythmic system because it can produce oscillations at two distinct periods (Barone and Paternó 1982). Birhythmicity is encountered in some biochemical Abou-Jaoudé *et al.* (2011b) and non-linear electronic systems (Yamapi *et al.* 2010; Ghosh *et al.* 2011; Yamapi *et al.* 2012; Yue *et al.* 2012). In JJ physics, it is encountered in arrays coupled through an external circuit that possesses resonances (Likharev 1986). In the literature, it is well known that the junctions are hysteretic, and hence can be considered birhythmic, which is capable of oscillating at different frequencies for the same set of parameters. In this regard, Pountougnigni *et al.* (2019) presented the effects of uncorrelated white noise, in a series of JJs coupled to a linear RLC resonator.

Kingni *et al.* (2020) analysed the aspect of JJ with TNB. Nana *et al.* (2018) investigated the dynamics of an RLC series circuit with a hysteretic iron-core inductor, and not limited to Yamapi and Filatrella (2014) who investigated the effect of noise on a JJ that is coupled to a linear RLC resonator. Based on this literature and to the best of our knowledge, there is no work in the literature on the analytical and numerical analysis of an RCSJJ with TNB coupled to a linear RLC resonator. This paper is aimed at investigating the analytical and numerical analyses of an RCSJJ with TNB coupled to a linear RLC resonator. This leads to the following specific objectives: To model and analyse an RCSJJ with TNB coupled to a linear RLC resonator and to characterise the dynamical behaviours exhibited by an RCSJJ with TNB coupled to a linear RLC resonator. This paper is divided into three sections. Section 1 deals with the introduction of the paper. Section 2 presents the rate equations and theoretical analyses of the RCSJJ with TNB coupled to a linear RLC resonator. Finally, Section 3 presents the conclusion.

THEORETICAL ANALYSIS OF THE RCSJJ WITH A TNB COUPLED TO A LINEAR RLC RESONATOR

The RCSJJ with TNB coupled to a linear RLC resonator is an electrical circuit depicted in Fig. 1.
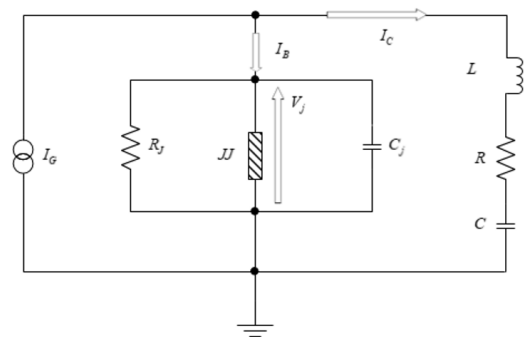

Figure 1 Equivalent electric circuit of the RCSJJ with TNB coupled to a linear RLC resonator.

Applying Kirchhoff's current and voltage laws to the schematic of Fig. 1, one has the following set of equations:

$$\begin{cases} I_G = I_{R_J} + I_J + I_C + I, \\ V_J = V_R + V_L + V_C, \\ V_J = \dfrac{\hbar}{2e}\dfrac{d\phi}{dt} \end{cases} \quad (1)$$

where $I_{R_J}, I_J = I_{J_C}\sin\phi + I_{UCPR}\sin\left(\frac{\phi}{2}\right)$ and I_C are the currents through the resistor across the junction, the JJ, and the capacitor across the junction respectively. I_{J_C} is the critical current of the junction, and $\phi = \phi_2 - \phi_1$ is the gauge-invariant phase difference across the two superconductors. Also, V_R, V_L, V_C, and I are the voltages across the resistor, inductor, capacitor, and the current on the RLC loop respectively and by substituting the various expressions of the currents and the expression of the voltages in the system (1), the following system (2) is obtained:

$$I_G = \frac{\hbar C_J}{2e}\frac{d^2\phi}{dt^2} + \frac{\hbar}{2eR_J}\frac{d\phi}{dt} + I_{J_C}\sin\phi + I_{UCPR}\sin\left(\frac{\phi}{2}\right) + \frac{d\tilde{q}}{dt}, \quad (2)$$

$$\frac{d^2\tilde{q}}{dt^2} + \frac{R}{L}\frac{d\tilde{q}}{dt} - \frac{\hbar}{2eL}\frac{d\phi}{dt} + \frac{1}{CL}\tilde{q} = 0. \quad (3)$$

Introducing the following dimensionless parameters,

$$\omega_o = \sqrt{\frac{2eI_{JC}}{\hbar C_J}}, \quad \tau = \omega_o t, \quad q = \omega_o \tilde{q}/I_{JC},$$

$$\alpha = \frac{1}{R_J}\sqrt{\frac{\hbar}{2eI_{JC}C_J}}, \quad \beta_L = \frac{2eI_{JC}L}{\hbar}, \quad \Omega = \frac{1}{\omega_o\sqrt{LC}}, \quad \sigma = \frac{R}{L\omega_o},$$

$$m = \frac{I_{UCPR}}{I_{JC}}, \quad \gamma_G = \frac{I_G}{I_{JC}},$$

the normalized form of the system (2) is as follows:

$$\begin{cases} \dfrac{d^2\phi}{d\tau^2} + \alpha\dfrac{d\phi}{d\tau} + \sin\phi + m\sin\left(\dfrac{\phi}{2}\right) + \dfrac{dq}{d\tau} = \gamma_G, \\ \dfrac{d^2q}{d\tau^2} + \sigma\dfrac{dq}{d\tau} - \dfrac{1}{\beta_L}\dfrac{d\phi}{d\tau} + \Omega^2 q = 0 \end{cases} \quad (4)$$

It is interesting to note that the parameters; γ_G is the applied current, Ω is the resonant frequency, and β_L is the perturbed frequency of the junction, and the fractional parameter $m(m \geq 0)$ represents the contribution of 2π–periodic Josephson current for $m = 0$ or 2π–periodic Josephson current and 4π–periodic Josephson current for $0 < m \leq 1$. The current phase relation of the Josephson current cannot take into account only periodic the 4π–Josephson current. Therefore, it is a particular case of the current-phase relation used in [56]. Letting $v = \frac{d\phi}{d\tau}$ and $i = \frac{dq}{d\tau}$ system (3) is transformed into a system of first-order ordinary differential equations given by:

$$\frac{dv}{d\tau} = \gamma_G - \alpha v - i - \sin\phi - m\sin\left(\frac{\phi}{2}\right), \quad (5)$$

$$\frac{di}{d\tau} = \frac{1}{\beta_L}v - \sigma i - \Omega^2 q, \quad (6)$$

$$\frac{d\phi}{d\tau} = v, \quad (7)$$

$$\frac{dq}{d\tau} = i. \quad (8)$$

System (4) is the mathematical transformation of the schematic of Fig. 1 representing the RCSJJ with TNB coupled to a linear RLC resonator.

Stability analysis of the RCSJJ with TNB couple to a linear RLC resonator

The stability of the system is done by characterising the equilibrium points of the system. This is done by solving the system (4) for; $\frac{d\phi}{d\tau} = 0$, $\frac{dv}{d\tau} = 0$, $\frac{dq}{d\tau} = 0$, and $\frac{di}{d\tau} = 0$. By this resolution of the equilibrium points $E_i(v^*, i^*, \phi^*, q^*)$ system (4) is characterised by different values of the fractional parameters m which elaborate on the various states in which the system exists. When the fractional parameter $m = 0$, system (4) reduces to:

$$v^* = 0; \quad i^* = 0; \quad q^* = 0, \quad (9)$$

$$\gamma_G - \sin\phi^* = 0, \quad (10)$$

as shown in [57], with two solutions $E_1(0, 0, \arcsin(i), 0)$ and $E_2(0, 0, \pi - \arcsin(i), 0)$ for $\gamma_G \leq 1$, and no solution for $\gamma_G > 1$. The associated characteristic equation is given by:

$$\lambda^4 + b_3\lambda^3 + b_2\lambda^2 + b_1\lambda + b_0 = 0, \quad (11)$$

where

$$b_3 = \sigma + \alpha; \quad b_2 = \frac{\Omega^2\beta_L + \alpha\beta_L + \beta_L\cos(\phi^*) + 1}{\beta_L};$$

$$b_1 = \alpha\Omega^2 + \sigma\cos(\phi^*); \quad b_0 = \Omega^2\cos(\phi^*).$$

For a system to be stable, it is necessary and sufficient that each turn of the first column of the Routh array must be positive. If this condition is not met, the system is unstable and the numbers of sign changes in the first column correspond to the number of roots of the characteristic equation in the right half of the S-plane. The first column of the Routh array for system (6) is given by the coefficients of the d_i given by $d_1 = b_3$; $d_2 = \frac{b_3 b_2 - b_1}{b_3}$; $d_3 = b_1 + \frac{b_0 b_3}{d_2}$; $d_4 = b_0$. After analysis, it is found that the equilibrium point E_1 is unconditionally stable while the equilibrium point E_2 is unstable.

When the fractional parameter is $0 < m \leq 1$, the resolution of the system (4) is given by:

$$v^* = 0; \quad i^* = 0; \quad q^* = 0, \quad (12)$$

$$\gamma_G - \sin\phi^* - m\sin\left(\frac{\phi^*}{2}\right) = 0. \quad (13)$$

System (7) is a nonlinear system in ϕ^*, which the solution can only be approximated via a numerical method say the Newton-Raphson method. By this, the system depicts no roots, two or four roots as a function of the value of parameters ($\gamma_G = i_{dc}, m$) as shown in Fig. 2.

The characteristic equation of system (4) evaluated at the equilibrium points $E_i(0, 0, \phi^*, 0)$ is given by Eqn. (6) with the following:

$$b_3 = \sigma + \alpha;$$

$$b_2 = \frac{1}{2}\left(\frac{m\beta_L\cos\left(\frac{\phi^*}{2}\right) + 2\Omega^2\beta_L + 2\sigma\alpha\beta_L + 2\beta_L\cos(\phi^*) + 2}{\beta_L}\right);$$

$$b_1 = \alpha\Omega^2 + \sigma\cos(\phi^*) + \frac{1}{2}\sigma m\cos\left(\frac{\phi^*}{2}\right);$$

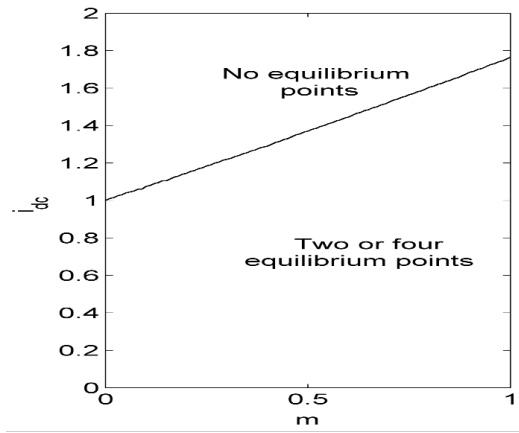$$b_0 = \frac{1}{2}\Omega^2\left(m\cos\left(\frac{\phi^*}{2}\right) + 2\cos(\phi^*)\right).$$

Figure 2 Repartition of equilibrium points of system (4) in the parameter space spanned by m and $\gamma_G = i_{dc}$.

Given credit to the Routh-Hurwitz stability criterion, the real parts of all the roots λ of Eqn. (6) are negative if and only if: $d_1 = b_3$; $d_2 = \frac{b_3 b_2 - b_1}{b_3}$; $d_3 = b_1 + \frac{b_0 b_3}{d_2}$; $d_4 = b_0$ are all greater than zero, or else the system is unstable.

Numerical analysis of the RCSJJ with TNB couple to a linear RLC resonator

The influence of the nontrivial barrier will be investigated in this section numerically. Figure 3 presents the voltage-intensity curves for different values of the parameter m.
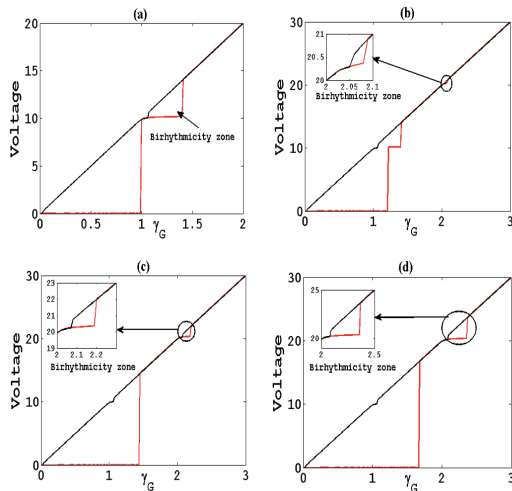

Figure 3 Voltage-intensity curves for different values of m: m_1, m_2, m_3, m_4. The red solid line represents the increasing current bias and the black solid line represents the decreasing current bias. The inset shows the birhythmicity zone for the RCSJJ with the TNB (m_5). The parameters of simulations are: α, β, γ, δ.

In Figure 3 (a) for $m = m_1$, the resonant step locked to the cavity is more detailed in the range $1.05 < \gamma_G < 1.40$ where the system stays on one or the other frequency, depending on the initial conditions (that are controlled by the bias sweep) [58]. The relevant feature is that the system remains birhythmic for any value of m as shown in Fig. 3 (b) to (d). Another feature inferred by the fractional parameter is the coexistence of two resonant state intervals for m bounded between m_2 and m_3. Therefore one realizes that the first

resonant state interval $\gamma_G = \gamma_{G1}$ is still on the diagram and is slightly destroyed as m increases (see Fig. 3 (b)). The destruction of the former is followed simultaneously by the appearance of the new resonant state interval. The total disappearance of the first resonant state interval is evident when m is set beyond the value m_4 (see Fig. 3 (c) and Fig. 3 (d)). The latter is enlarged with the increase of m. The hysteresis on the new resonant state interval confers to the system the birhythmic properties. Figure 4 shows the projection of phase space in the (x, y) plane and the time evolution of the charge resonator for different values of parameter m. The birhythmic behaviour is characterized by the existence of two limit cycles depending on initial conditions. Each attractor can be identified by its amplitude and frequency.
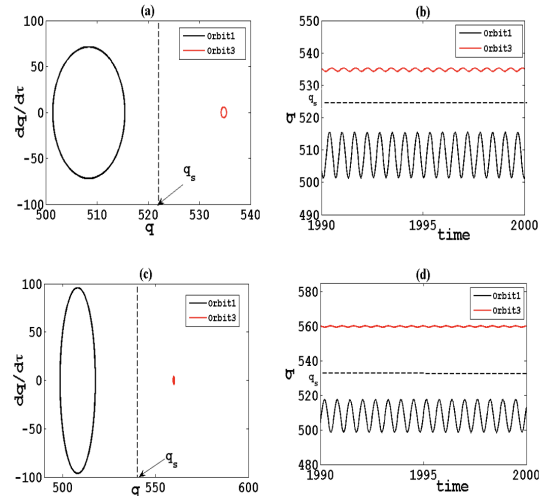

Figure 4 (a) and (b) Projection of phase space in $q - \frac{dq}{d\tau}$ plane and time evolution respectively for $m = 0.6$ and $\gamma_G = 2.15$; (c) and (d) projection of phase space in $q - \frac{dq}{d\tau}$ plane and time evolution respectively for $m = 0.9$ and $\gamma_G = 2.25$. The parameters of the simulation are $\alpha = 0.1$, $\beta_L = 0.01$, $\Omega = 2.0$, $Q = 200.0$.

Figure 4 is associated with the attractor with large excursion in charge oscillations with frequency Ω_1 and to the other attractor the frequency Ω_3 which is stable. One can estimate the existence of an unstable orbit with the frequency Ω_2 between the two which is indicated on the diagram by the guessed position q_s of the separatrix. Regarding the curves on the diagram, the role that can be assigned to the parameter m is described as follows: the orbit with the frequency Ω_1 sees its amplitude increasing with the increase of the parameter m while the amplitude of the orbit with frequency Ω_2 tends to smaller values. Another way of analyzing is to set the variation of the amplitude of voltage and the amplitude of charge when the bias is swept. We define the amplitude as the large excursion of the phase derivative $\frac{d\phi}{d\tau}$ (which is proportional to the JJ voltage) and the charge q (which is proportional to the capacitor voltage). Therefore, we set:

$$A = \max_\tau \frac{d\phi}{d\tau} - \min_\tau \frac{d\phi}{d\tau}, \tag{14}$$

$$B = \max_\tau q - \min_\tau q. \tag{15}$$

The amplitude diagram versus the bias current γ_G for many values of the parameter m is shown in Figs. 5 and 6.
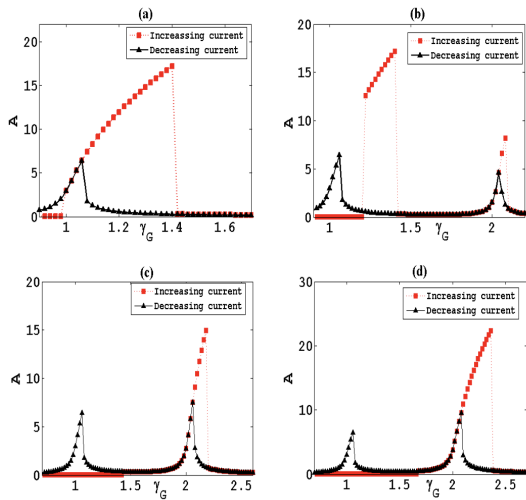

Figure 5 Amplitude A as a function of the bias current γ_G for many values of the parameter m: (a) $m = 0$, (b) $m = 0.3$, (c) $m = 0.6$, (d) $m = 0.9$. Squares refer to increasing the bias current and the triangles to decreasing the bias current which is equivalent to the voltage oscillations across the JJ. The parameters of simulations are the same as in Fig. 2.
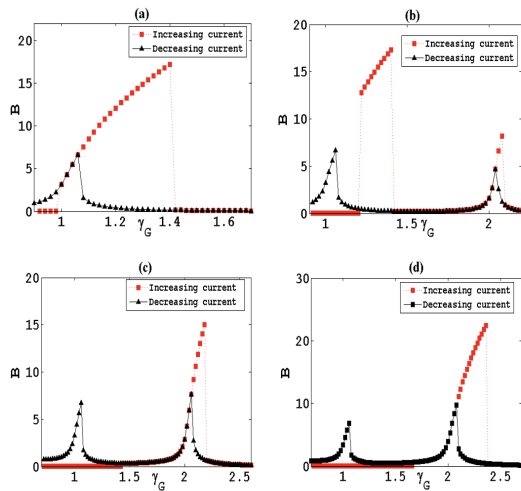

Figure 6 Amplitude B as a function of the bias current γ_G for many values of the parameter m: (a) $m = 0$, (b) $m = 0.3$, (c) $m = 0.6$, (d) $m = 0.9$. Squares refer to increasing the bias current and triangles refer to decreasing the bias current which is equivalent to the voltage of the capacitor. The parameters of simulations are the same as in Fig. 2.

CONCLUSION

This paper was devoted to the analytical and numerical analyses of an RCSJJ with a TNB coupled to a linear RLC resonator. The modelling and numerical investigation of the RCSJJ with TNB coupled to a linear RLC resonator were studied. The rate equations describing RCSJJ with TNB coupled to the RLC resonator are established by using Kirchhoff's current and voltage laws. The system was characterized by four, two, or no equilibrium points depending on the external direct current (DC) source and the fractional parameter.

The stability analysis of the equilibrium points with credit to the Routh-Hurwitz stability criterion reveals that the stability of equilibrium points depends on the system's parameters. Current-voltage characteristic reveals the presence of the birhythmicity zone which is sensitive to the fractional parameter m. As the fractional parameter increases, the coexistence of the resonant state is destroyed, which is followed simultaneously by the appearance of a new resonance state. Depending on initial conditions, birhythmic behaviour is characterized by the existence of period-1-attractors. The projection of the phase space in the specific plane and the time evolution of charge is predicted in which the amplitude of attractors reported are sensitive to the fractional parameter.

LITERATURE CITED

Abou-Jaoudé, W., M. Chaves, and J.-L. Gouzé, 2011a A theoretical exploration of birhythmicity in the p53-mdm2 network. PLoS One **6**: e17075.

Abou-Jaoudé, W., M. Chaves, and J.-L. Gouzé, 2011b A theoretical exploration of birhythmicity in the p53-mdm2 network. PLoS One **6**: e17075.

Aleiner, I. L. and Y. M. Blanter, 2002 Inelastic scattering time for conductance fluctuations. Phys. Rev. B **65**: 1–10.

Bao, R., L. Huang, Y. Lai, and C. Grebogi, 2015 Conductance fluctuations in chaotic bilayer graphene quantum dots. Phys. Rev. E **012918**: 1–8.

Barone, A. and G. Paternó, 1982 *Physics and applications of the Josephson effect*. Wiley and Sons, New York.

Bee, G., K. Ballentine, and M. Thomsen, 2008 Realistic problems involving thermal conductivity. Am. J. Phys. **76**: 970–974.

Belli, F., T. Novoa, J. Contreras-García, and I. Errea, 2012 Strong correlation between electronic bonding network and critical temperature in hydrogen-based superconductors. Nat. Commun. **12**: 1–11.

Campi, D., S. Kumari, and N. Marzari, 2021 Prediction of phonon-mediated superconductivity with high critical temperature in the two-dimensional topological semimetal w2n3. Nano Lett. **21**: 3435–3442.

Canturk, M. and I. N. Askerzade, 2013 Chaotic dynamics of externally shunted josephson junction with unharmonic cpr. J. Supercond. Nov. Magn. **26**: 839–843.

Casagrande, V. and A. S. Mikhailov, 2005 Birhythmicity, synchronization, and turbulence in an oscillatory system with nonlocal inertial coupling. Phys. D Nonlinear Phenom. **205**: 154–169.

Clarke, J. and F. K. Wilhelm, 2008 Superconducting quantum bits. Nature **453**: 1031–1042.

Decroly, O. and A. Goldbeter, 1982 Birhythmicity, chaos, and other patterns of temporal self-organization in a multiply regulated biochemical system. Proc. Natl. Acad. Sci. USA **79**: 6917–6921.

Dominguez, F., F. Hassler, and G. Platero, 2012 Dynamical detection of majorana fermions in current-biased nanowires. Phys. Rev. B **86**: 1405031–5.

Eck, R., D. Scalapino, and B. Taylor, 1965 Low-temperature physics ix. In *9th International Conference*, edited by J. G. e. a. Daunt, p. 415, Plenum Press, Inc.

Filatrella, G., G. Rotoli, N. Gro/nbechJensen, R. D. Parmentier, and N. F. Pedersen, 1992 Model studies of long josephson junction arrays coupled to a high-q resonator. Journal Appl. Phys. **72**: 3179–3185.

Fu, L. and C. L. Kane, 2009 Josephson current and noise at a superconductor/quantum-spin-hall-insulator/superconductor junction. Phys. Rev. B **79**: 161408.

Fujii, T., S. H. Matsuo, K. Takashima, N. Hatakenaka, S. Kurihara, *et al.*, 2009 Theoretical studies on dynamical casimir effect in a superconducting artificial atom. In *QFEXT09 (University Oklahoma, USA)*, edited by K. A. Milt and M. Bordag, p. 344, World Scientific.

Geva-zatorsky, N. *et al.*, 2006 Oscillations and variability in the p53 system. Mol. Syst. Biol. pp. 1–13.

Ghosh, P., S. Sen, S. S. Riaz, and D. S. Ray, 2011 Controlling birhythmicity in a self-sustained oscillator by time-delayed feedback. Phys. Rev. E **83**: 36205.

González, H., H. Arce, and M. R. Guevara, 2008 Phase resetting, phase locking, and bistability in the periodically driven saline oscillator: Experiment and model. Phys. Rev. E **78**: 36217.

Grib, A. *et al.*, 2006 Synchronization of serial intrinsic josephson junction arrays on vicinal substrates. Supercond. Sci. Technol. **19**: S200–S204.

Gross, B. *et al.*, 2013 Modeling the linewidth dependence of coherent terahertz emission from intrinsic josephson junction stacks in the hot-spot regime. Phys. Rev. B **88**: 14524.

Haberichter, T., M. Marh, and R. Heinrich, 2001 Birhythmicity, trirhythmicity and chaos in bursting calcium oscillations. Biophys. Chem. **90**: 17–30.

Hadley, P., M. R. Beasley, and K. Wiesenfeld, 1988 Phase locking of josephson-junction series arrays. Phys. Rev. B **38**: 8712–8719.

Hounsgaard, B. Y. J., H. Hultborn, B. Jespersen, and O. Kiehn, 1988 Bistability of alpha-motoneurones in the decerebrate cat and in the acute spinal cat after intravenous 5-hydroxytryptophan. J. Physiol. **405**: 345–367.

Kadji, H. E., J. C. Orou, R. Yamapi, and P. Woafo, 2007 Nonlinear dynamics and strange attractors in the biological system. Chaos, Solitons & Fractals **32**: 862–882.

Kingni, S. T., A. Cheukem, A. C. Chamgoué, and F. T. Kamga, 2020 Analysis of josephson junction with topologically nontrivial barrier. Eur. Phys. J. B **93**: 143–147.

Kingni, S. T., G. F. Kuiate, V. K. Tamba, A. V. Monwanou, J. Bio, *et al.*, 2019 Analysis of a fractal josephson junction with unharmonic current-phase relation. Supercond. Nov. Magn. **32**: 2295–2301.

Kleiner, R., D. Koelle, F. Ludwig, and J. Clarke, 2004 Superconducting quantum interference devices. state of art and applications. In *Proceedings of the IEEE*, volume 92, p. 1534.

Likharev, K. K., 1986 *Dynamics of Josephson junction and circuits*.

Gordon Breach, New York.

Lima, F. C. E., A. R. Moreira, L. E. Machado, and C. A. S. Almeida, 2021 Statistical properties of linear majorana fermions. Int. J. Quantum Chem. **121**: e26749.

McDermott, R., S. Lee, B. T. Haken, A. H. Trabesinger, A. Pines, *et al.*, 2004 Microtesla mri with a superconducting quantum interference device. Proc. Natl. Acad. Sci. **101**: 7857–7861.

Morita, M., K. Iwamoto, and M. Sen, 1989 Transition sequence and birhythmicity in a chemical oscillation model showing chaos. Phys. Rev. A **40**: 6592–6596.

Mourik, V., K. Zou, S. M. Frolov, S. R. Plissard, E. P. A. M. Bakkers, *et al.*, 2012 Signatures of majorana fermions in hybrid superconductor-semiconductor nanowire devices. Science **336**: 1003–1007.

Nana, B., S. B. Yamgoué, I. Kemajou, R. Tchitnga, and P. Woafo, 2018 Dynamics of an rlc series circuit with hysteretic iron-core inductor. Chaos, Solitons and Fractals **106**: 184–192.

Nori, F., 2008 Designing quantum-information-processing superconducting qubit circuits that exhibit lasing and other atomic-physics-like phenomena on a chip. In *APS March Meeting Abstracts*, pp. H15–001.

Oladapo, B. I., S. A. Zahedi, S. C. Chaluvadi, S. S. Bollapalli, and M. Ismail, 2018 Model design of a superconducting quantum interference device of magnetic field sensors for magnetocardiography. Biomed. Signal Process. Control **46**: 116–120.

Ovchinnikov, Y. N. and V. Z. Kresin, 2013 Networks of josephson junctions and their synchronization. Phys. Rev. B **88**: 214504.

Owen, C. S. and D. J. Scalapino, 1997 Inductive coupling of josephson junctions to external circuits. J. Appl. Phys. **2047**.

Ozyuzer, L. *et al.*, 2007 Emission of coherent thz radiation from superconductors. Science (80-.) **318**: 1291–1293.

Pountougnigni, O. V., R. Yamapi, G. Filatrella, and C. Tchawoua, 2019 Noise and disorder effects in a series of birhythmic josephson junctions coupled to a resonator. arXiv **3**: 1–13.

Ramakrishnan, B., A. A. Oumate, M. Tuna, Koyuncu, S. T. Kingni, *et al.*, 2022 Analysis, fpga implementation of a josephson junction circuit with topologically nontrivial barrier and its application to ring-based dual entropy core true random number generator. Eur. Phys. J. Spec. Top. **231**: 1049–1059.

Sosnovtseva, O. V., D. Setsinsky, A. Fausboll, and E. Mosekilde, 2002 Transitions between beta and gamma rhythms in neural systems. Phys. Rev. E **66**: 41901.

Stich, M., M. Ipsen, and A. S. Mikhailov, 2002 Self-organized pacemakers in birhythmic media. Phys. D Nonlinear Phenom. **171**: 19–40.

Veldhorst, M., C. G. Molenaar, C. J. M. Verwijs, H. Hilgenkamp, and A. Brinkman, 2012 Optimizing the majorana character of squids with topologically nontrivial barriers. Phys. Rev. B **86**: 024509–1075.

Ventura, A. *et al.*, 2007 Restoration of p53 function leads to tumour regression in vivo. Nature **445**: 661–665.

Wang, H. B. *et al.*, 2010 Coherent terahertz emission of intrinsic josephson junction stacks in the hot spot regime. Phys. Rev. Lett. **105**: 57002.

Wen, X.-G., 2006 Topological orders and edge excitations in fractional quantum hall states. Adv. Phys. **44**: 405–473.

Wendin, G., 2017 Quantum information processing with superconducting circuits: a review. Reports Prog. Phys. **80**: 1060011–50.

Xie, H.-Y. and A. Levchenko, 2019 Topological supercurrents interaction and fluctuations in the multiterminal josephson effect. Phys. Rev. B **99**: 0945191–9.

Yamapi, R. and G. Filatrella, 2014 Noise effects on birhythmic

josephson junction coupled to a resonator. Phys. Rev. E **89**.

Yamapi, R., G. Filatrella, and M. A. Aziz-Alaoui, 2010 Global stability analysis of birhythmicity in a self-sustained oscillator. Chaos **20**: 1–12.

Yamapi, R., G. Filatrella, M. A. Aziz-Alaoui, and H. A. Cerdeira, 2012 Effective fokker-planck equation for birhythmic modified van der pol oscillator. Chaos **22**: 1–10.

Yue, X., W. Xu, L. Wang, and B. Zhou, 2012 Transient and steady-state responses in a self-sustained oscillator with harmonic and bounded noise excitations. Probabilistic Eng. Mech. **30**: 70–76.

Zakharova, A., T. Vadivasova, V. Anishchenko, A. Koseska, and J. Kurths, 2010 Stochastic bifurcations and coherence like resonance in a self-sustained bistable noisy oscillator. Phys. Rev. E **81**: 11106.

How to cite this article: Metsebo, J., Abdou, B., Ngatcha, D. T., Ngongiah, I. K., Kuate, P. D. K., and Pone, J. R. M. Analysis of a resistive-capacitive shunted Josephson junction with topologically nontrivial barrier coupled to a RLC resonator. *Chaos and Fractals*, 1(1), 31-37, 2024.